



Parameter based definition of eccentric cycloid gearings

Stefan Landler¹ · Maximilian Trübswetter¹ · Michael Otto¹ · Karsten Stahl¹

Received: 10 March 2023 / Accepted: 11 May 2023 / Published online: 7 June 2023
© The Author(s) 2023

Abstract

Current challenges for today's industry are an increase in gear ratio in one stage, an increase in load capacity as well as an increase in efficiency compared to standard gears. The standard tooth profile for cylindrical gears is an involute. This tooth profile has certain limits for external gearings regarding its geometry, e.g., undercutting and a small radius of curvature near the base circle. Special gearings overcome these limits and offer an enormous potential in gear design through their adapted profile geometries. New manufacturing possibilities for gears, such as additive manufacturing or 5-axis milling, mean that special gears can also be produced economically.

In comparison to involute gears the description of non-involute gears is often not standardized and parameters describing the geometry are not commonly defined. Thus, it is not possible to adequately determine the corresponding properties. One of these special tooth profiles is the eccentric cycloid gearing (EC gearing), in which a circular profile rolls with a profile of a trochoid equidistant. This flank geometry can provide advantages over the standard involute in certain applications. This study introduces a geometric description of the EC gearing, which is based on a defined set of parameters. Besides the geometrical parameters, parameters describing the characteristics of the gearing are proposed in accordance with the description of involute gears. This parametric description of the EC gearing enables an analytical determination of the flank, the contact geometry and load-free characteristics. With the parametric description shown and the variation of the geometry possible with it, gearings suitable for practical applications can be generated.

Parameterbasierte Definition von Exzenter-Zykloiden-Verzahnungen

Zusammenfassung

Für die heutige Industrie ist das Offenlegen von Potenzial hinsichtlich einer höheren Übersetzung in einer Stufe, einer Erhöhung der Tragfähigkeit sowie einer Wirkungsgradsteigerung im Vergleich zu Standardverzahnungen wichtig. Evolventenverzahnungen stellen die aktuell bedeutendste Verzahnungsart für Stirnräder im Maschinenbau dar. Durch dieses Verzahnungsprofil bestehen bei Außenverzahnungen aber auch gewisse Probleme wie die Mindestzähnezahl zur Vermeidung von Unterschnitt und die kleinen Krümmungsradien in der Nähe des Grundkreises. Sonderverzahnungen können durch ihre angepassten Profilgeometrien diese Potenziale heben. Durch die neuen Herstellmöglichkeiten von Zahnrädern, wie beispielsweise additive Fertigung oder 5-Achs-Fräsen, können auch Sonderverzahnungen wirtschaftlich erzeugt werden. Im Gegensatz zur Evolventenverzahnung ist die Beschreibung von Sonderverzahnungen oftmals nicht standardisiert und die notwendigen Parameter zur Beschreibung der Geometrie sind nicht einheitlich definiert. Dadurch ist es nicht möglich, die entsprechenden Verzahnungsparameter geeignet zu bestimmen. Eine dieser Sonderverzahnungen ist die Exzenter-Zykloiden-Verzahnung (EZ-Verzahnung), bei welcher ein Kreisprofil mit einem Profil einer Trochoidenäquidistante abwälzt. Durch diese Flankengeometrie können Vorteile gegenüber der standardmäßigen Evolvente in bestimmten Anwendungsfällen entstehen.

Availability of data and material 'Not applicable'

Code availability 'Not applicable'

✉ Stefan Landler
stefan.landler@tum.de

¹ Gear Research Center (FZG), School of Engineering and Design, Technical University of Munich, Boltzmannstraße 15, 85748 Garching bei München, Germany

Diese Veröffentlichung führt die geometrische Beschreibung der EZ-Verzahnung anhand eines definierten Parametersatzes ein. Neben den geometrischen Parametern werden auch Kennwerte zur Beschreibung der Verzahnungscharakteristiken eingeführt, welche sich an der Beschreibung der Evolventenverzahnung orientieren. Dadurch diese parametrische Beschreibung der EZ-Verzahnung ist es möglich, die Flanken- und Kontaktgeometrie sowie die lastfreien Charakteristiken analytisch zu bestimmen. Mit der aufgezeigten parametrischen Beschreibung und der damit möglichen Variation der Geometrie können in der Praxis anwendungsgerechte Verzahnungen erzeugt werden.

1 Introduction

The most commonly used tooth profile of cylindrical gears in industrial engineering is the involute. The involute gearing has certain limits for external cylindrical gears, such as a low minimum number of teeth and high contact pressure near the base circle. Special gearings can avoid these disadvantages by an adjusted geometry and achieve an improvement of the gear characteristics for certain applications. Modern manufacturing capabilities also allow the advantages of special gears to be implemented economically and precisely. These processes include 5-axis milling [1] and additive manufacturing [2].

The eccentric cycloid gearing (EC gearing) is a special gearing which uses an eccentric circular arc profile on one gear. This allows extremely low numbers of teeth to be achieved down to the single-tooth pinion, see Fig. 1a. The mating gear has an equidistant of a roulette as the flank profile according to the law of gearing. Due to the circular arc profile, the shape of the roulette is a cycloidal curve. The cycloidal curve is also called a trochoid [3]. Figure 1a shows a closed form of the cycloidal curve which represents the flanks of the gear for the meshing with a single-toothed pinion.

Based on the descriptions of the geometry, a general definition of EC gearing can be given. The EC gearing is defined by the meshing of a gear with a circular arc profile with a gear with a tooth profile of an equidistant of a trochoid. For external cylindrical gears, this definition is applied to the transverse section. The following study refers only to this type of gears. The gear with the circular arc profile is called an arc gear, the gear with the profile of an equidistant of a trochoid a cycloid gear.

With this definition, the different number of teeth of the arc gear z_1 can be chosen. Figure 1b shows an arc gear with $z_1 = 2$, Fig. 1c a gearing with $z_1 = 12$. The number of teeth of the mating cycloid gear is $z_2 = 6$ for Fig. 1a and b and $z_2 = 15$ for Fig. 1c.

Figure 1 shows the different geometries possible for an EC gearing with the same center distance a . For the possibility of comparing the EC gearing with the established involute gearing, a detailed description of the geometry is necessary. This allows the characteristics of comparable gears with different profiles to be examined and evaluated.

2 State of the art

A gearing consisting of a gear with circular arc profile and a gear with the tooth profile of an equidistant of a trochoid is already described in early gear design literature. Authors of standard literature such as Niemann and Winter [4] and Linke et al. [5] describe the basic principle of this gearing under the name cylindrical lantern gear. The exact geometry and gear characteristics are not described in detail. Another type of gearing similar to the EC gearing is the Grisson gearing [6]. In this case, an extremely low number of teeth of the cycloid gear is usually selected with a higher number of teeth of the arc gear. In this case, as well, only the structure is described in the literature without a detailed analysis of the geometry.

One of the first descriptions of the geometry of a gearing with the name EC gearing is given by Stanovskoy et al. [7]. Here, the structure of an EC gearing with a single-toothed arc gear is described. Contact patterns of this EC gearing with a single-toothed pinion and deviations of the center distance are shown by Kazakyavichyus et al. [8]. Li et al. [9] describe the details of the geometry of an EC gearing with a single-toothed arc gear and analyze the undercutting conditions. Li et al. [9] study the tooth contact in terms of the radius of curvature, the contact lines, and the surface of action. They also present results of a loaded tooth contact analysis performed with the finite element method. Batsch et al. [10] apply flank modifications to the EC gearing and determine the ease-off and transmission errors. They also provide comparisons to involute gearing and Wildhaber-Novikov gearing. Stanovskoy et al. describe in different patents [11–14] the structure of the EC gearing in different designs and applications. A detailed analysis of the geometry is not performed.

The additive manufacturing of a multiple-toothed EC gearing together with a basic description of the geometry is shown by Batsch [15]. Bubenchikov et al. [16] describe a profile cutter for the manufacturing of an EC gearing. Shcherbakov et al. [17] use envelopes for the manufacturing of the EC gearing with a milling process. A possible application for EC gearing is shown by Dubov et al. [18] in the transmission of a geokhod for boring.

For the description of the geometry of the EC gearing, many different methods can be used. The method by Johann and Scheurle [19] can be used in particular to determine the

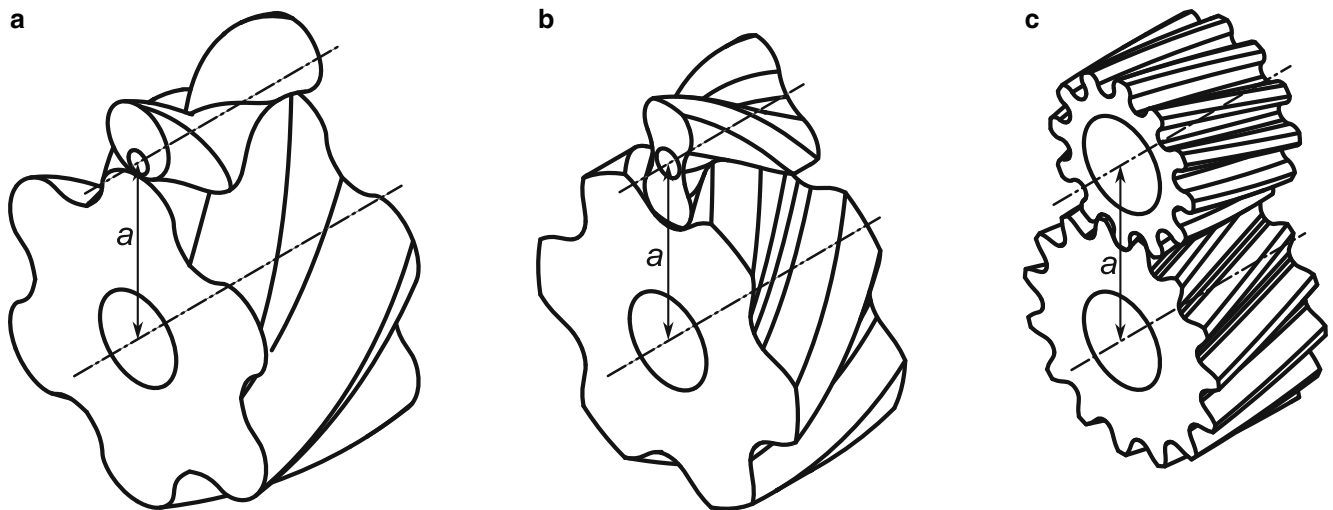


Fig. 1 Different EC gearings with the same center distance (a: $z_1 = 1, z_2 = 6$. b: $z_1 = 2, z_2 = 6$; c: $z_1 = 12, z_2 = 15$)

geometry of special gearings. Based on the given geometry of a gear, the geometry of the mating gear is determined with the aid of differential equations derived from the law of gearing. Zimmer et al. [20] show the application of this method to the geometry of an EC gearing with the known geometry of a single-tooth arc gear. An independent description of the two gears is not possible with the method by Johann and Scheurle [19]. Another method of describing the trochoid and its equidistant is shown by Lehmann [21]. The analytical derivation of the curve geometry allows an independent description of the two meshing flanks. Lehmann [21] does not show the complete geometry of a gear, but limits to the curves.

Overall, the literature shows that a complete description of all partial geometries of an arbitrary EC gearing is currently not available. Therefore, this study presents a parameter-based description of the EC gearing, which can be used for further analyses. The developed geometry is used to determine various load-free characteristics.

3 Analytical description of the geometry

For an analytical description of the EC gearing, the individual parts of the geometry must be considered. The first step is to determine the flank geometry of the arc gear. This is represented by a circular arc profile. According to Fig. 2 the vector \vec{p}_{PA} from the center of the arc gear O_1 to the point on the circular arc profile P_A can be calculated using the position of the center of the arc profile O_A . Therefore,

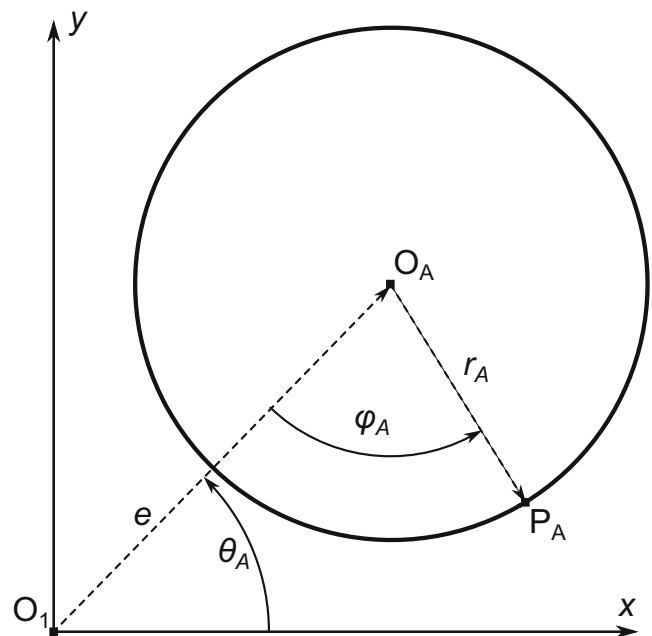


Fig. 2 Structure of the circular arc profile of the arc gear

it results using the eccentricity e of the circular arc profile to the gear origin and its arc radius r_A :

$$\begin{aligned} \vec{p}_{PA} &= \begin{pmatrix} x_{PA} \\ y_{PA} \end{pmatrix} \\ &= e \cdot \begin{pmatrix} \cos(\Theta_A) \\ \sin(\Theta_A) \end{pmatrix} - r_A \cdot \begin{pmatrix} \cos(\Theta_A + \varphi_A) \\ \sin(\Theta_A + \varphi_A) \end{pmatrix} \end{aligned} \tag{1}$$

x_{PA} is the x-component, y_{PA} the y-component of the vector \vec{p}_{PA} . θ_A is the angle of arc position, φ_A the angle of arc profile. With Eq. 1, the transverse section of the single-tooth arc gear from Fig. 1a is completely described.

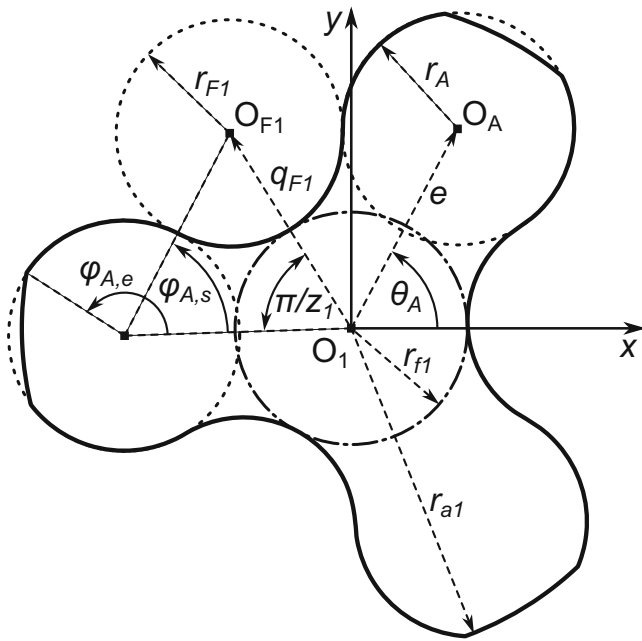


Fig. 3 Structure of the arc gear with multiple circular arcs

For multi-tooth gears, the description must be extended. Figure 3 shows the transverse section of an arc gear with three teeth. The right and left flanks of one tooth in this case are described by the same circle. This represents a special case, which is used as a starting point for further considerations. The teeth are connected by a circular fillet, which is common for optimizing the load capacity of gears [22] and has advantages over trochoidal fillets especially for small numbers of teeth [23]. The transition between the circular arc of the flank and the fillet profile is tangential and is defined by the starting angle of the arc profile $\varphi_{A,s}$, see Fig. 3. The arc profile is limited towards the tooth tip by the ending angle of the arc profile $\varphi_{A,e}$. The tip radius r_{a1} can be calculated with:

$$r_{a1} = e - r_A \cdot \cos(\varphi_{A,e}) \tag{2}$$

The reference diameter d_1 of the arc gear is defined by the reference radius r_1 . The reference radius r_1 is identical to the eccentricity e :

$$d_1 = 2 \cdot r_1 = 2 \cdot e \tag{3}$$

All centers of the arc profiles of one arc gear must be on the reference circle to fulfil the law of gearing. This ensures a uniform transmission ratio. The module is a common reference parameter for involute gears, which is also implemented as a reference parameter for the EC gearing.

The module m is defined in accordance with the transverse module from ISO 21771 [24]:

$$m = \frac{d_1}{z_1} = \frac{2 \cdot e}{z_1} \tag{4}$$

With the same underlying circle for both flanks, the radius of the arc profile determines the tooth thickness. A radius $r_{A,equal}$ can be determined with the law of cosines where the tooth thickness is equal to the space width. This radius $r_{A,equal}$ is adjusted by the factor r_A^* to the intended arc radius r_A :

$$r_A = r_A^* \cdot r_{A,equal} = r_E^* \cdot e \cdot \sqrt{2 - 2 \cdot \cos\left(\frac{\pi}{2 \cdot z_1}\right)} \tag{5}$$

With this definition of the arc radius factor, its influence on the geometry can be determined. The factor must be greater than zero. An upper limit depends on the remaining geometry parameters. With a factor $r_A^* = 1.0$ the tooth thickness at the reference circle is equal to the space width.

The assumption made above that the two flanks of one tooth are described by the same circle is generalized in the following. The two flanks are thus described independently of each other. Figure 4 shows an arc gear, where each flank is described by its own circular arc profile. The condition remains that the center of each profile must be located on the reference circle. In the following, symmetri-

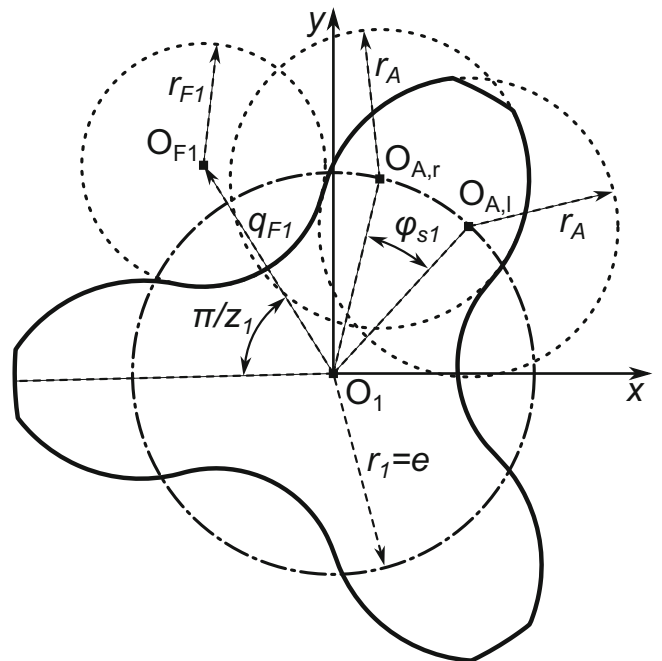


Fig. 4 Structure of the arc gear with varying circular arc profiles

cal gear teeth are required, so the radius of each arc profile must be identical. The angle between the flank centers $O_{A,l}$ and $O_{A,r}$ is called tooth thickness angle φ_{sl} and is composed of two separate influences:

$$\varphi_{s1} = \varphi_{rA} + \varphi_{jl} \tag{6}$$

φ_{rA} is the angle between the arc profiles without backlash and φ_{jl} is the backlash angle. With the separation of these two angles, the backlash angle can be applied to the arc gear alone. The definition of the backlash angle φ_{jl} is according to ISO 21771 [24]. φ_{rA} describes the angle between the arc profiles of the left and the right flank of one tooth which is needed to adjust a certain tooth thickness without backlash. The tooth thickness on the reference circle can be adjusted with the factor s_t^* . The following equation results from the law of cosines:

$$\varphi_{rA} = 2 \cdot \arccos\left(\frac{2 \cdot e^2 - r_A^2}{2 \cdot e^2}\right) - s_t^* \cdot \frac{\pi}{z_1} \tag{7}$$

According to this definition, the tooth thickness factor is in the range of 0 to 2. The influence on the geometry can be shown by means of individual extreme cases for backlash-free gearings ($\varphi_{jl} = 0$): In case of $s_t^* = 0$, the tooth thickness at the reference circle is zero. The space width at the reference circle, on the other hand, becomes zero for the boundary case of $s_t^* = 2$. For $s_t^* = 1$, the tooth thickness is equal to the space width at the reference circle. Thus, the factor enables an adjustment of the gearing according to a complementary gearing [5, 25]. If the tooth thickness factor fits the following equation, the centers of the flanks are identical ($\varphi_{rA} = 0$):

$$s_t^* = \frac{2 \cdot z_1}{\pi} \cdot \arccos\left(\frac{2 \cdot e^2 - r_A^2}{2 \cdot e^2}\right) \tag{8}$$

The tooth root is designed as a circular fillet as described above. With the description of the flank geometry shown, the distance q_{F1} of the center of the circular fillet profile O_{F1} to the gear center O_1 can be calculated using the law of sines:

$$q_{F1} = e \cdot \frac{\sin(\varphi_{A,s})}{\sin\left(\pi \cdot \left(\frac{z_1 - 1}{z_1}\right) - \varphi_{A,s} - \frac{\varphi_{rA}}{2}\right)} \tag{9}$$

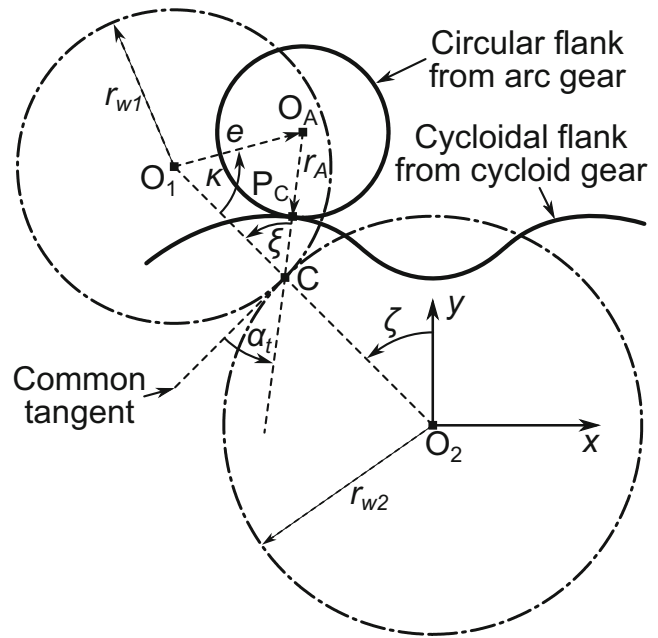


Fig. 5 Structure of the cycloid gear based on the meshing with the arc profile

The determined distance q_{F1} can be used to calculate the fillet radius r_{F1} of a tangential circle using the law of cosines:

$$r_{F1} = \sqrt{e^2 + q_{F1}^2 - 2 \cdot e \cdot q_{F1} \cdot \cos\left(\frac{\pi}{z_1} + \frac{\varphi_{rA}}{2}\right)} - r_A \tag{10}$$

With the description of the fillet geometry, the root diameter d_{f1} as well as the root radius r_{f1} can be determined as follows:

$$d_{f1} = 2 \cdot r_{f1} = 2 \cdot (q_{F1} - r_{F1}) \tag{11}$$

The geometry of the arc gear is thus described completely in terms of parameters. According to the method of Lehmann [21], the geometry of the circular arc profile of the arc gear is used to generate the flank geometry of the cycloid gear. Figure 5 shows the flank contact in detail. The transmission ratio i is crucial for the meshing of the two gears of the EC gearing. This is determined by the number of teeth [4]:

$$i = \frac{z_2}{z_1} \tag{12}$$

The geometry of a cycloidal curve is strongly determined by the trochoid ratio λ , which is defined with the pitch radius of the arc gear r_{w1} according to [26]:

$$\lambda = \frac{e}{r_{w1}} \tag{13}$$

The trochoid ratio determines whether the resulting trochoid is a normal ($\lambda = 1$), shortened ($\lambda < 1$), or elongated ($\lambda > 1$) cycloid. For the EC gearing, usually only the trochoid with $\lambda < 1$ is used.

The pitch radius of the cycloid gear r_{w2} can be determined with the transmission ratio i :

$$r_{w2} = i \cdot r_{w1} \tag{14}$$

This results in the calculation of the pitch radius of the arc gear r_{w1} with the center distance a :

$$r_{w1} = \frac{a}{1 + i} \tag{15}$$

The center distance a can therefore be determined as follows:

$$a = r_{w1} + r_{w2} = e \cdot \frac{1 + i}{\lambda} \tag{16}$$

For the design of EC gearings, the specification of the center distance a and the trochoid ratio λ is more convenient. Therefore, the module m can be determined as follows:

$$m = 2 \cdot a \cdot \frac{\lambda}{z_1 + z_2} \tag{17}$$

The generation of the cycloidal curve is initiated by the angle of revolution ζ , see Fig. 5. This angle describes the revolution of the arc profile around the center O_2 of the stationary cycloid gear. According to the rolling condition, a rotation of the circular arc profile around the center O_1 results. The rotation angle κ can thus be determined from the transmission ratio i according to:

$$\kappa = i \cdot \zeta \tag{18}$$

The point vector \vec{p}_{OA} is determined by vector addition:

$$\begin{aligned} \vec{p}_{OA} &= \begin{pmatrix} x_{OA} \\ y_{OA} \end{pmatrix} \\ &= a \cdot \begin{pmatrix} -\sin(\zeta) \\ \cos(\zeta) \end{pmatrix} - e \cdot \begin{pmatrix} -\sin(\zeta + \kappa) \\ \cos(\zeta + \kappa) \end{pmatrix} \end{aligned} \tag{19}$$

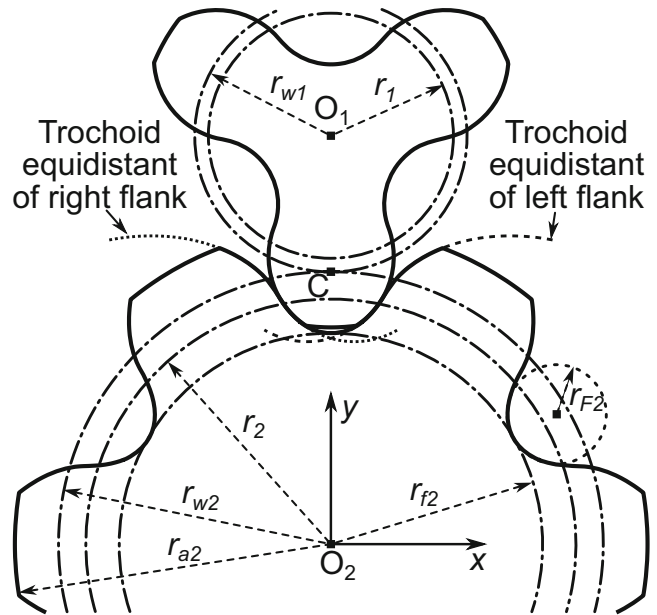


Fig. 6 Structure of the cycloid gear meshing with an arc gear with varying arc profiles

x_{OA} is the x-component, y_{OA} the y-component of the vector \vec{p}_{OA} . The point O_A moves on a trochoid. The point P_C moves on an equidistant curve to this trochoid. The point vector \vec{p}_{PC} is determined by vector addition with the vector $\vec{O_A P_C}$ which is normal to the trochoid and points in the direction of the pitch point C :

$$\begin{aligned} \vec{p}_{PC} &= \begin{pmatrix} x_{PC} \\ y_{PC} \end{pmatrix} = \vec{p}_{OA} + \vec{O_A P_C} \\ &= a \cdot \begin{pmatrix} -\sin(\zeta) \\ \cos(\zeta) \end{pmatrix} - e \cdot \begin{pmatrix} -\sin(\zeta + \kappa) \\ \cos(\zeta + \kappa) \end{pmatrix} \\ &\quad - r_A \cdot \begin{pmatrix} -\sin(\zeta - \xi) \\ \cos(\zeta - \xi) \end{pmatrix} \end{aligned} \tag{20}$$

x_{PC} is the x-component, y_{PC} the y-component of the vector \vec{p}_{PC} . The contact angle ξ describes the rotation of the normal vector around the pitch point C and can be calculated using trigonometry:

$$\begin{aligned} \xi &= \arctan\left(\frac{e \cdot \sin(\kappa)}{r_{w1} - e \cdot \cos(\kappa)}\right) \\ &= \arctan\left(\frac{\lambda \cdot \sin(\kappa)}{1 - \lambda \cdot \cos(\kappa)}\right) \end{aligned} \tag{21}$$

Due to the alignment of the vector $\vec{O_A P_C}$ in the direction of the pitch point C , the law of gearing is always fulfilled.

Figure 6 shows the structure of the cycloid gear with different circular arc profiles for the individual flanks of the arc gear. Here, two different trochoid equidistants are formed, representing the two flanks. The backlash angle is not con-

Table 1 Set of parameters to describe the EC gearing

Designation	Symbol
Number of teeth of arc gear	z_1
Number of teeth of cycloid gear	z_2
Center distance	a
Helix angle of arc gear	β_1
Facewidth	b
Trochoid ratio	λ
Starting angle of arc profile	$\varphi_{A,s}$
Ending angle of arc profile	$\varphi_{A,e}$
Arc radius factor	r_A^*
Tooth thickness factor	S_t^*
Tip clearance factor	c^*
Backlash angle of arc gear	φ_{j1}

sidered here for the two generating circular arc profiles. This means that the resulting EC gearing has backlash. The complete cycloid gear can be generated from the two curves of the trochoid equidistants. The necessary boundaries for this can be derived from the arc gear.

The reference diameter of the cycloid gear d_2 can be calculated with the module m :

$$d_2 = m \cdot z_2 \tag{22}$$

The limitation of the flank curves is determined by the tip clearance c of the gearing. The tip clearance c is defined by a tip clearance factor c^* and the module m :

$$c = c^* \cdot m \tag{23}$$

For involute gears, the tip clearance factor is usually $c^* = 0.25$ [5]. Thus, the root diameter d_{f2} can be calculated as follows:

$$d_{f2} = 2 \cdot \left(a - \frac{d_{a1}}{2} - c \right) \tag{24}$$

Using this root diameter, a tangential circle with radius r_{F2} can be fitted to the two trochoid equidistants. The tip diameter d_{a2} is calculated analogous to the root diameter d_{f2} :

$$d_{a2} = 2 \cdot \left(a - \frac{d_{f1}}{2} - c \right) \tag{25}$$

The geometry of the cycloid gear in the transverse section is therefore completely defined. In order to generate helical EC gearing the helix angle β is introduced. According to Linke et al. [5], the helix angle of the cycloid gear β_2 is the negative value of the helix angle of the arc gear β_1 :

$$\beta_2 = -\beta_1 \tag{26}$$

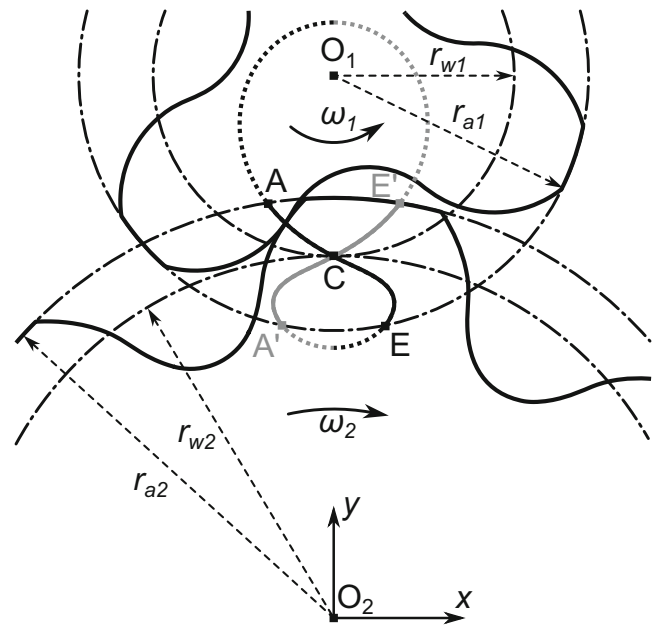


Fig. 7 Details of the meshing between the arc gear and the cycloid gear

This equation can be applied to all cylindrical gears. According to ISO 21771 [24], the overlap angle φ_β defines the relative angle of the two faces of a gear. The angle $\varphi_{\beta 1}$ of the arc gear is given by the facewidth b :

$$\varphi_{\beta 1} = 2 \cdot b \cdot \frac{\tan(\beta_1)}{d_1} \tag{27}$$

The convention here is that a positive helix angle for external gears results in a positive overlap angle about the z-axis [4, 5]. A positive helix angle thus leads to right-handed gear teeth for external gears. It follows thus for the angle $\varphi_{\beta 2}$ of the cycloid gear:

$$\varphi_{\beta 2} = 2 \cdot b \cdot \frac{\tan(\beta_2)}{d_2} = -2 \cdot b \cdot \frac{\tan(\beta_1)}{d_2} = -\frac{\varphi_{\beta 1}}{i} \tag{28}$$

Now the complete geometry of the three-dimensional EC gearing is defined. All necessary parameters for the EC gearing can be summarized in Table 1.

The parameters from this table can be used to create arbitrary EC gearings.

4 Meshing of the EC gearing

The details of the tooth contact of the EC gearing with the corresponding path of contact are shown in Fig. 7. The rotation direction of the gears is represented by the angular velocities ω_1 and ω_2 . The black line around the pitch point C shows the path of contact when the arc gear is driving. Point A shows the start of the meshing, point E the end

Table 2 Exemplary set of parameters of the EC gearing for following calculations

Parameter	Symbol	Numerical value	Unit
Number of teeth of arc gear	z_1	3	–
Number of teeth of cycloid gear	z_2	6	–
Center distance	a	100	mm
Helix angle of arc gear	β_1	25	°
Facewidth	b	80	mm
Trochoid ratio	λ	0.97	–
Starting angle of arc profile	$\varphi_{A,s}$	60	°
Ending angle of arc profile	$\varphi_{A,e}$	170	°
Arc radius factor	r_A^*	1.0	–
Tooth thickness factor	S_t^*	1.0	–
Tip clearance factor	c^*	0.1	–
Backlash angle of arc gear	φ_{j1}	1.0	°

of the meshing. The dotted line represents the path of action and thus the maximum possible path of contact. The limitation occurs at the respective tip circles. The grey line around the pitch point C shows the path of contact when the cycloid gear is driving. The path of contact is mirrored to the case of the driving arc gear. The two paths of action together give the shape of a distorted lemniscate, which is typical for any EC gearing.

The mathematical description of the path of action is similar to the description of the trochoid equidistant and is achieved by vector addition. In contrast to Eq. 20, the angle ζ is neglected. It follows for the point vector \vec{p}_{poa} from the center of the cycloid gear O_2 to the path of action:

$$\vec{p}_{poa} = \begin{pmatrix} x_{poa} \\ y_{poa} \end{pmatrix} = a \cdot \begin{pmatrix} 0 \\ 1 \end{pmatrix} - e \cdot \begin{pmatrix} -\sin(\kappa) \\ \cos(\kappa) \end{pmatrix} - r_A \cdot \begin{pmatrix} -\sin(-\xi) \\ \cos(-\xi) \end{pmatrix} \quad (29)$$

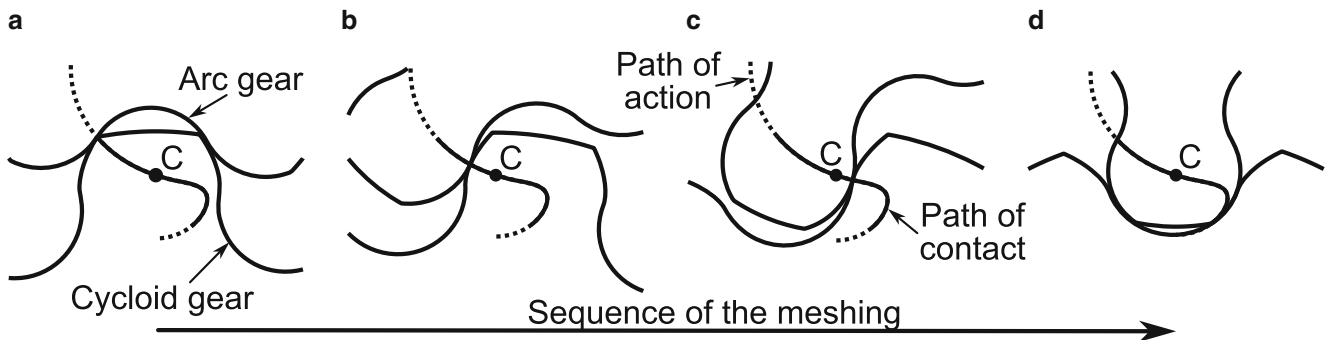


Fig. 8 Sequence of meshing of the exemplary EC gearing

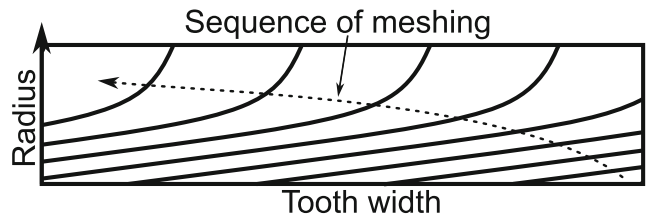


Fig. 9 Sequence of the line of contact on the arc gear flank (view on the flank surface)

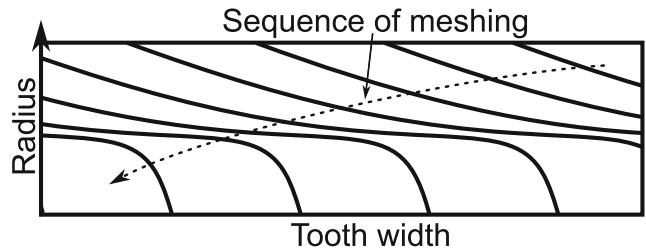


Fig. 10 Sequence of the line of contact on the cycloid gear flank (view on the flank surface)

x_{poa} is the x-component, y_{poa} the y-component of the vector \vec{p}_{poa} . The path of action can also be referenced to the center of the arc gear O_1 shifting it by the center distance a .

For further analyses, an exemplary EC gearing is chosen. The parameters of this gearing can be seen in Table 2.

The geometry generated with this can be used to represent the meshing of the EC gearing. Figure 8 shows four different meshing positions with the arc gear driving and rotating counterclockwise. Figure 8a shows the beginning of the meshing, Fig. 8d shows the end.

Especially noticeable in Fig. 8 is the strongly curved path of contact at the end of the meshing. The reason for this is the osculation of the two tooth flanks in this area.

The two-dimensional calculation of the path of contact can also be used for the three-dimensional determination of the line of contact. Thereby, a width-variable angle $\zeta(z)$ must be used for the calculation of the angles κ and ξ . The

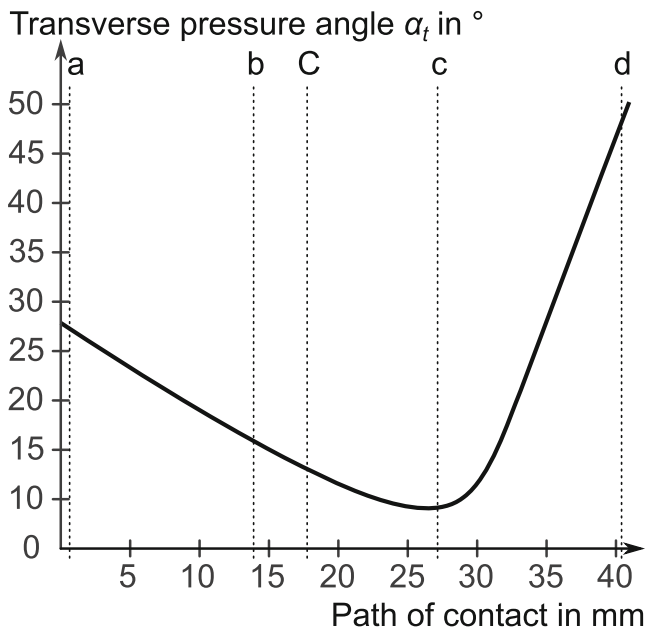


Fig. 11 Transverse pressure angle over the path of contact of the exemplary EC gearing

angle $\zeta(z)$ depends on the facewidth coordinate z and is determined analogous to Eq. 28:

$$\zeta(z) = \zeta_s + z \cdot \frac{2 \cdot \tan(\beta)}{i \cdot d_2} \tag{30}$$

ζ_s represents the starting angle of the gear face. The contact lines thus determined depend on the meshing position and can be projected onto the flanks of the arc gear and cycloid gear. Figure 9 shows the sequence of the line of contact projected onto the flank of the arc gear with the configuration of Fig. 8. The strong curvature of the path of contact at the end of the meshing results in the curvature of the line of contact at the tooth tip.

Figure 10 shows the sequence of the line of contact projected onto the flank of the cycloid gear with the configuration of Fig. 8. Here, the curvature of the contact line at the tooth root is a result of the curvature of the path of contact at the end of meshing.

5 Determination of load-free characteristics

The calculated geometry of the EC gearing can be used to determine certain characteristics. In this study, only load-free characteristics, which are determined on conjugate and non-deformed flanks are considered. The most important characteristics are the contact conditions, represented by pressure angle, sliding and radius of curvature.

5.1 Pressure angle

The transverse pressure angle α_t describes the angle of the normal vector on the flanks in relation to the common tangent of the pitch circles, see Fig. 5. The transverse pressure angle can be calculated with:

$$\alpha_t = \frac{\pi}{2} - \xi \tag{31}$$

The pressure angle describes the direction of the contact force in the overall transmission. A changing value therefore leads to changing reaction forces in the gear components, e.g., in the bearings. A large pressure angle also results in the radial forces from the tooth contact becoming exceptionally large.

Figure 11 shows the transverse pressure angle for the EC gearing with the configuration of Fig. 8. A minimum pressure angle is shown in the area of the meshing position of Fig. 8c. The maximum pressure angle is at the end of the meshing.

5.2 Sliding factor

The sliding velocity v_g of the gearing can be calculated with the velocities of each flank at the contact point. The velocities of the flank can be determined using the angular velocities. Here, a three-dimensional view is necessary. The vector of angular velocity of the arc gear $\vec{\omega}_1$ with the angular velocity ω_1 is defined as follows:

$$\vec{\omega}_1 = \begin{pmatrix} 0 \\ 0 \\ \omega_1 \end{pmatrix} \tag{32}$$

Analogous to this, the vector of angular velocity of the cycloid gear $\vec{\omega}_2$ considering the transmission ratio i :

$$\vec{\omega}_2 = \begin{pmatrix} 0 \\ 0 \\ -\frac{\omega_1}{i} \end{pmatrix} \tag{33}$$

These vectors can be used to determine the velocity of the flanks. For the velocity \vec{v}_1 of points on the flank of the arc gear, the path of action must be referenced to the center of the arc gear. It follows:

$$\begin{aligned} \vec{v}_1 &= \begin{pmatrix} v_{1,x} \\ v_{1,y} \\ v_{1,z} \end{pmatrix} = \vec{\omega}_1 \times \left(\vec{p}_{\text{poa}} - \begin{pmatrix} 0 \\ a \\ 0 \end{pmatrix} \right) \\ &= \begin{pmatrix} 0 \\ 0 \\ \omega_1 \end{pmatrix} \times \left(-e \cdot \begin{pmatrix} -\sin(\kappa) \\ \cos(\kappa) \\ 0 \end{pmatrix} - r_A \cdot \begin{pmatrix} -\sin(-\xi) \\ \cos(-\xi) \\ 0 \end{pmatrix} \right) \end{aligned} \tag{34}$$

$v_{1,x}$ is the x-component, $v_{1,y}$ the y-component and $v_{1,z}$ the z-component of the vector \vec{v}_1 . Analogous for the mating gear, the velocity \vec{v}_2 of points on the flank of the cycloid gear is:

$$\begin{aligned} \vec{v}_2 &= \begin{pmatrix} v_{2,x} \\ v_{2,y} \\ v_{2,z} \end{pmatrix} = \vec{\omega}_2 \times \vec{p}_{poa} \\ &= \begin{pmatrix} 0 \\ 0 \\ -\frac{\omega_1}{i} \end{pmatrix} \times \left(\mathbf{a} \cdot \begin{pmatrix} 0 \\ 1 \\ 0 \end{pmatrix} - \mathbf{e} \cdot \begin{pmatrix} -\sin(\kappa) \\ \cos(\kappa) \\ 0 \end{pmatrix} \right) \\ &\quad - r_A \cdot \begin{pmatrix} -\sin(-\xi) \\ \cos(-\xi) \\ 0 \end{pmatrix} \end{aligned} \tag{35}$$

$v_{2,x}$ is the x-component, $v_{2,y}$ the y-component and $v_{2,z}$ the z-component of the vector \vec{v}_2 .

The circumferential velocity v_t is the Euclidian norm of the vector \vec{v}_C , which is the velocity of the pitch point C. This results in the following for v_t :

$$\begin{aligned} v_t &= |\vec{v}_C| = |\vec{\omega}_1 \times \vec{O_1C}| = \left| \begin{pmatrix} 0 \\ 0 \\ \omega_1 \end{pmatrix} \times \begin{pmatrix} 0 \\ -r_{w1} \\ 0 \end{pmatrix} \right| \\ &= \omega_1 \cdot r_{w1} \end{aligned} \tag{36}$$

The velocity $v_{1/2,t}$ in the direction of the common tangent of the flanks is a part of the velocity calculated in Eq. 34 and 35. The common tangent can be determined using the transverse pressure angle α_t .

In the case of a driving arc gear, the tangential velocity $v_{1/2,t}$ is given by:

$$\begin{aligned} v_{1/2,t} &= \left\langle \vec{v}_{1/2}, \begin{pmatrix} \sin(\alpha_t) \\ \cos(\alpha_t) \\ 0 \end{pmatrix} \right\rangle \\ &= v_{1/2,x} \cdot \sin(\alpha_t) + v_{1/2,y} \cdot \cos(\alpha_t) \end{aligned} \tag{37}$$

The velocity in the direction of the common normal is zero according to the law of gearing [19]. The sliding velocity v_g can be determined from the difference between the tangential velocity of the driving ($v_{driving,t}$) and driven ($v_{driven,t}$) gear:

$$v_g = v_{driving,t} - v_{driven,t} \tag{38}$$

In the case of a driving arc gear:

$$v_g = (v_{1,x} - v_{2,x}) \cdot \sin(\alpha_t) + (v_{1,y} - v_{2,y}) \cdot \cos(\alpha_t) \tag{39}$$

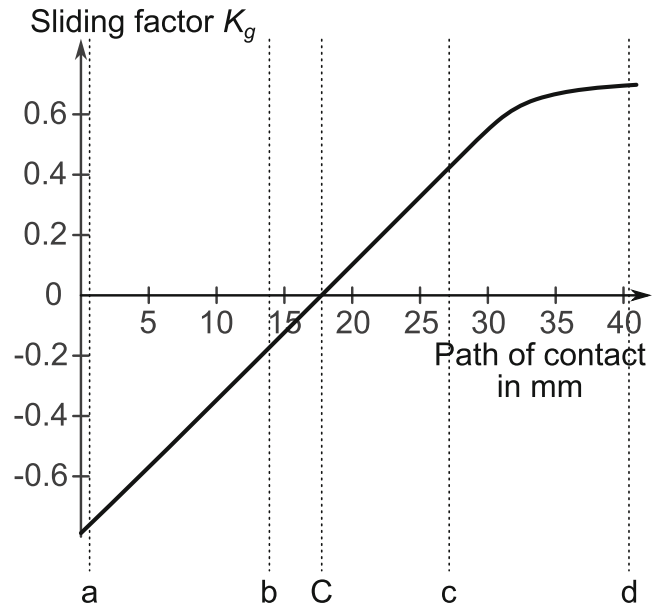


Fig. 12 Sliding factor over the path of contact of the exemplary EC gearing

With these calculated velocities, the sliding factor K_g can be determined:

$$K_g = \frac{v_g}{v_t} \tag{40}$$

The sliding factor K_g is thus a dimensionless quantity for assessing the sliding velocity v_g of a gearing. The sliding factor can be used to evaluate the gearing in terms of heating and scuffing [5]. Figure 12 shows the sliding factor for the EC gearing with the configuration of Fig. 8. A correlation between the curvatures of the path of action and the course of the sliding factor can be seen.

5.3 Radius of curvature

The radius of curvature is needed to calculate the flank pressure according to the theory of Hertz. It is defined that a positive radius corresponds to a convex flank and a negative radius to a concave flank. The EC gearing is defined in the transverse section, the radii of curvature are also determined in the transverse section. The radius of curvature of the arc gear $\rho_{1,t}$ is specified with the radius of the arc profile r_A :

$$\rho_{1,t} = r_A \tag{41}$$

The radius of curvature of the cycloid gear $\rho_{2,t}$ can be calculated as the radius of curvature of a plane curve. This curve is the trochoid equidistant of the cycloid gear. The derivative of the trochoid equidistant with respect to the

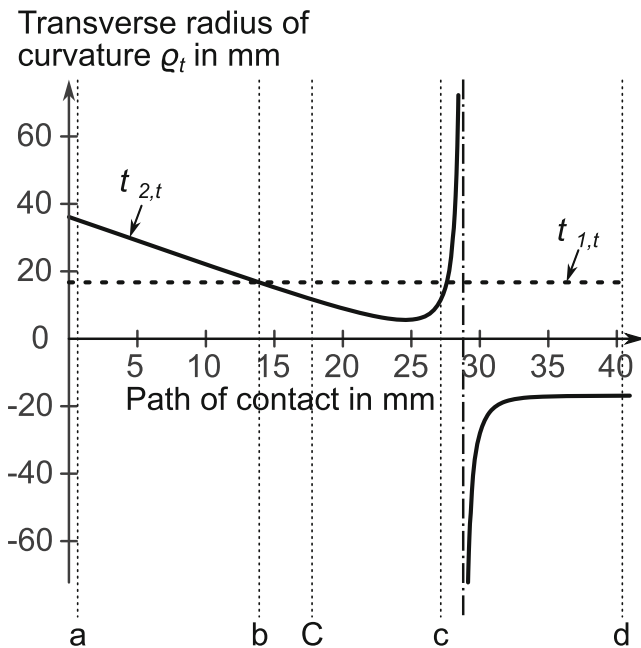


Fig. 13 Transverse radius of curvature of both gears over the path of contact of the exemplary EC gearing

angle ζ can be simplified with the derivative of the trochoid with respect to the angle ζ . Some transformations result in the following equation:

$$\begin{aligned} \rho_{2,t} &= \frac{\left(\left(\frac{\partial x_{PC}}{\partial \zeta} \right)^2 + \left(\frac{\partial y_{PC}}{\partial \zeta} \right)^2 \right)^{\frac{3}{2}}}{\frac{\partial x_{PC}}{\partial \zeta} \cdot \frac{\partial^2 y_{PC}}{\partial \zeta^2} - \frac{\partial^2 x_{PC}}{\partial \zeta^2} \cdot \frac{\partial y_{PC}}{\partial \zeta}} \\ &= \frac{\left(\left(\frac{\partial x_{OA}}{\partial \zeta} \right)^2 + \left(\frac{\partial y_{OA}}{\partial \zeta} \right)^2 \right)^{\frac{3}{2}}}{\frac{\partial x_{OA}}{\partial \zeta} \cdot \frac{\partial^2 y_{OA}}{\partial \zeta^2} - \frac{\partial^2 x_{OA}}{\partial \zeta^2} \cdot \frac{\partial y_{OA}}{\partial \zeta}} - r_A \\ &= a \cdot \frac{(1 + \lambda^2 - 2 \cdot \lambda \cdot \cos(\kappa))^{\frac{3}{2}}}{1 + \lambda^2 \cdot (1 + i) - \lambda \cdot (2 + i) \cdot \cos(\kappa)} - r_A \end{aligned} \tag{42}$$

Figure 13 shows the radii of curvature for the EC gearing with the configuration of Fig. 8. It can be seen that the curvature of the arc gear is uniform. The curvature of the cycloid gear, on the other hand, shows strong variations over the meshing. At the beginning of the meshing the flank is convex, at the end it is concave. Near the meshing position c, the radius of curvature becomes infinite, so there is an inflection point of the flank geometry. This inflection point is an asymptote of Eq. 42. The position of this asymptote can be calculated with:

$$\zeta = \frac{1}{i} \cdot \arccos \left(\frac{1 + \lambda^2 \cdot (1 + i)}{\lambda \cdot (2 + i)} \right) \tag{43}$$

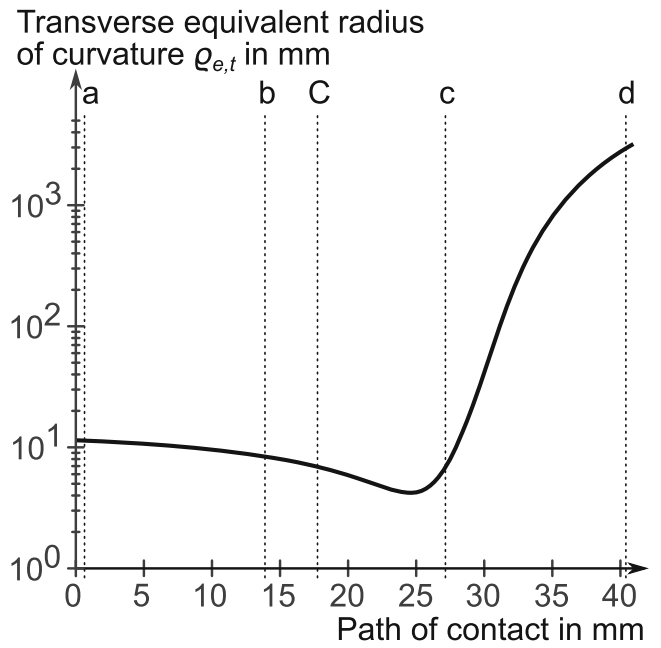


Fig. 14 Transverse equivalent radius of curvature over the path of contact of the exemplary EC gearing

The equivalent radius of curvature $\rho_{e,t}$ evaluates the contact condition for a calculation with respect to the theory of Hertz. The equivalent radius of curvature can be calculated with:

$$\rho_{e,t} = \frac{\rho_{1,t} \cdot \rho_{2,t}}{\rho_{1,t} + \rho_{2,t}} \tag{44}$$

Figure 14 shows the equivalent radius of curvature for the EC gearing with the configuration of Fig. 8. The ordinate of the graph shown in Fig. 14 is a logarithmic scale. It can be seen that a minimum of the equivalent radius of curvature exists, which is not directly recognizable from Fig. 13. At the end of the meshing, a large equivalent radius of curvature is evident, which can be attributed to the osculation of the flanks.

6 Conclusion

A detailed description of the geometry of the special gearings is necessary to determine and classify its characteristics. This allows potentials to be identified in comparison to the established involute gearing. This paper shows a parameter-based definition of the geometry of the EC gearing. The parameters are used for the complete description of the gear geometry and the determination of various characteristics derived from it. Options for setting a clearance for practice-relevant gearings are included.

The developed flank geometry is used to determine the meshing conditions. The sequence of the meshing in the

Table 3 Nomenclature

Symbols					
A	Starting point of meshing	a	Center distance	b	Facewidth
C	Pitch point	c	Tip clearance	c^*	Tip clearance factor
d	Reference diameter	D_a	Tip diameter	D_f	Root diameter
E	End point of meshing	e	Eccentricity	i	Transmission ratio
K_g	Sliding factor	m	Module	O	Center
P	Point	\vec{p}	Point vector	q_F	Root center distance
r	Reference radius	r_A	Arc radius	r_A^*	Arc radius factor
R_a	Tip radius	r_F	Circular fillet radius	R_f	Root radius
R_w	Pitch radius	S_t^*	Tooth thickness factor	\vec{v}	Velocity
V_g	Sliding velocity	V_t	Circumferential velocity	x	X-coordinate
y	Y-coordinate	z	Number of teeth, z-coordinate	α_t	Transverse pressure angle
β	Helix angle	ζ	Angle of revolution	θ_A	Angle of arc position
κ	Angle of rotation	λ	Trochoid ratio	ξ	Contact angle
Q_t	Transverse radius of curvature	$Q_{e,t}$	Transverse equivalent radius of curvature	φ_A	Angle of arc profile
φ_j	Backlash angle	φ_{rA}	Angle between arc profiles	φ_s	Tooth thickness angle
φ_β	Overlap angle	ω	Angular velocity	$\vec{\omega}$	Angular velocity vector
Indices					
l	Arc gear	2	Cycloid gear	A	Arc profile
C	Cycloid profile	Fl	Fillet of arc gear	$F2$	Fillet of cycloid gear
e	Ending point	l	Left flank	OA	Center of arc profile
PA	Point of arc profile	PC	Point of cycloid profile	Poa	Path of action
r	Right flank	s	Starting point	x	X-coordinate
y	Y-coordinate	z	Z-coordinate		

transverse section and on the flank surface is shown. The shape of the path of action and the lines of contact are discussed. Various load-free characteristic values are determined based on an exemplary EC gearing. The specifics of the pressure angle, sliding factor, and radii of curvature are discussed.

Further work will focus on the determination of load-dependent characteristics. The deformation of the gearing can be considered using analytical approaches [27]. For example, the elastic consideration of the gearing can allow load-related transmission errors to be determined [28]. Comparable geometries from practice can be used to assess the applicability of the EC gearing. Other types of gears, such as the worm gear [29], can be used here as well.

7 Nomenclature

The nomenclature is shown in Table 3.

Acknowledgements The presented results are based on the research project IGF no. 20549N/2 (FVA 864 I) undertaken by the Research Association for Drive Technology e.V. (FVA) supported by the German Federation of Industrial Research Associations e.V. (AiF) in the

framework of the Industrial Collective Research Program (IGF) by the Federal Ministry for Economic Affairs and Climate Action (BMWK) based on a decision taken by the German Bundestag. The authors would like to thank for the sponsorship and support received from the FVA, AiF and the members of the project committee.

Funding The presented results are based on the research project IGF no. 20549N/2 (FVA 864 I), which is supported by the German Federation of Industrial Research Associations e.V. (AiF).

Funding Open Access funding enabled and organized by Projekt DEAL.

Conflict of interest S. Landler, M. Trübswetter, M. Otto and K. Stahl declare that they have no competing interests.

Open Access This article is licensed under a Creative Commons Attribution 4.0 International License, which permits use, sharing, adaptation, distribution and reproduction in any medium or format, as long as you give appropriate credit to the original author(s) and the source, provide a link to the Creative Commons licence, and indicate if changes were made. The images or other third party material in this article are included in the article's Creative Commons licence, unless indicated otherwise in a credit line to the material. If material is not included in the article's Creative Commons licence and your intended use is not permitted by statutory regulation or exceeds the permitted use, you will need to obtain permission directly from the copyright holder. To view a copy of this licence, visit <http://creativecommons.org/licenses/by/4.0/>.

References

- Gu L, Xu J, Luo S (2016) The design of new cycloid gear with variable cross section and the research of end milling in five-axis machine tool. *Manuf Technol* 16:497–502. <https://doi.org/10.21062/ujep/x.2016/a/1213-2489/MT/16/3/497>
- Schmitt M, Kamps T, Siglmüller F et al (2020) Laser-based powder bed fusion of 16MnCr5 and resulting material properties. *Addit Manuf*. <https://doi.org/10.1016/j.addma.2020.101372>
- Hazewinkel M (1995) Cycloidal curve. In: Coproduct—Hausdorff—Young inequalities. *Encyclopaedia of mathematics*, vol 2. Springer Science+Business, Dordrecht, pp 70–71
- Niemann G, Winter H (2003) Getriebe allgemein, Zahnradgetriebe – Grundlagen, Stirnradgetriebe, 2nd edn. *Maschinenelemente*, vol 2. Springer, Berlin, Heidelberg
- Linke H, Börner J, Heß R (2016) Cylindrical gears: Calculation—Materials—Manufacturing. Carl Hanser, München
- Roser E (1901) Untersuchung des Grissongetriebes. Dissertation, Technische Hochschule Stuttgart
- Stanovskoy VV, Kazakyavichyus SM, Remneva TA et al (2009) Hochübersetzendes und überlastfähiges Getriebe. *Antriebstechnik*, vol 48
- Kazakyavichyus SM, Stanovskoy VV, Remneva TA et al (2011) Performance of eccentric-cycloid engagement with change in the interaxial distance: Modification of tooth configuration. *Russ Eng Res* 31:197–199. <https://doi.org/10.3103/S1068798X11030130>
- Li X, Li C, Chen B et al (2017) Design and investigation of a cycloid helical gear drive. *J Mech Sci Technol* 31:4329–4336. <https://doi.org/10.1007/s12206-017-0831-8>
- Batsch M, Wydrzyński D, Przesłowski Ł (2022) Tooth contact analysis of cylindrical gears with an unconventional tooth profile. *Adv Sci Technol Res J* 16:119–129. <https://doi.org/10.12913/22998624/152172>
- Stanovskoy VV, Kazakyavichyus SM, Remneva TA et al (2009) Toothed wheel gearing (variants) and a planetary toothed mechanism based thereon (variants): US-Patent(US8157691B2)
- Stanovskoy VV, Kazakyavichyus SM, Remneva TA et al (2011) Exzentrisch zyklode Einrastung von Zahnprofilen (verschiedene Ausführungsformen): EU-Patent(EP2530359A1)
- Stanovskoy VV, Kazakyavichyus SM, Remneva TA et al (2011) Exzenter-Zykloidverzahnung: EU-Patent(EP2532926B1)
- Stanovskoy VV, Kazakyavichyus SM, Remneva TA et al (2012) Eccentrically cycloidal engagement of toothed profiles having curved teeth: US-Patent(US8789437B2)
- Batsch M (2019) Rapid prototyping and tooth contact analysis of eccentric cycloid gear mesh. *J KONBiN* 49:369–382. <https://doi.org/10.2478/jok-2019-0019>
- Bubenchikov AM, Kazakyavichyus SM, Shcherbakov NR (2016) Mathematical simulation of a profile cutter as a surface of revolution. *IOP Conf Ser Mater Sci Eng* 124:1–6. <https://doi.org/10.1088/1757-899X/124/1/012095>
- Shcherbakov NR, Bubenchikov AM, Kazakavitschyus SM (2015) Mathematical modelling of an arch tooth surface as an envelope. *AMM* 756:442–446. <https://doi.org/10.4028/www.scientific.net/AMM.756.442>
- Dubov G, Trukhmanov D, Chegoshv A et al (2018) Substantiation of the need to create an eccentric cycloidal gearing transmission of geokhod. *E3s Web Conf*. <https://doi.org/10.1051/e3sconf/20184103008>
- Johann A, Scheurle J (2009) On the generation of conjugate flanks for arbitrary gear geometries. *GAMM* 32:61–79. <https://doi.org/10.1002/gamm.200910005>
- Zimmer M, Otto M, Stahl K (2016) Berechnung und Optimierung von Geometrie und Eingriffsverhalten von Zahnformen beliebiger Achslage: Vom Verzahnungsgesetz zur optimalen Auslegung. *Forsch Ingenieurwes* 80:1–16. <https://doi.org/10.1007/s10010-016-0201-1>
- Lehmann M (1981) Die Beschreibung der Zykloiden, ihrer Äquidistanten und Hüllkurven: unter besonderer Berücksichtigung der Planeten-Getriebe mit Zykloiden-Kurvenscheiben. Habilitation Thesis, TU München
- Zou T, Shaker M, Angeles J et al (2014) Optimization of tooth root profile of spur gears for maximum load-carrying capacity. In: *Proceedings of the ASME 2014 International Design Engineering Technical Conferences & Computers and Information in Engineering Conference, IDETC/CIE 2014*, 17.08.–20.08.2014, Buffalo, New York, USA <https://doi.org/10.1115/DETC2014-34568>
- Spitas C, Spitas V (2007) A FEM study of the bending strength of circular fillet gear teeth compared to trochoidal fillets produced with enlarged cutter tip radius. *Mech Based Des Struct Mach* 35:59–73. <https://doi.org/10.1080/15397730601182802>
- ISO (2007) Gears—Cylindrical involute gears and gear pairs—Concepts and geometry (ISO 21771)
- Roth K (1998) Zahnradtechnik Evolventen-Sonderverzahnungen zur Getriebeverbesserung: Evoloid-, Komplement-, Keilschräg-, Konische-, Konus-, Kronenrad-, Torus-, Wälzkolbenverzahnungen, Zahnrad-Erzeugungsverfahren. Springer, Berlin, Heidelberg
- Hsieh C-F, Hwang Y-W (2008) Tooth profile of a roots rotor with a variable trochoid ratio. *Math Comput Model* 48:19–33. <https://doi.org/10.1016/j.mcm.2007.08.008>
- Hochrein J-F, Otto M, Stahl K (2022) Fast tooth deflection calculation method and its validation. *Forsch Ingenieurwes* 86:845–859. <https://doi.org/10.1007/s10010-022-00598-8>
- Westphal C, Brimmers J, Brecher C (2021) Analysis of the operational behavior of a high-speed planetary gear stage for electric heavy-duty trucks in multi-body simulation. *Power Transm Eng* 15:46–54
- Heilemann J (2005) Tragfähigkeit und Wirkungsgrad bei unterschiedlichen Schnecken-Zahnflankenformen unter Berücksichtigung der Oberflächenhärte und Härtetiefe. Dissertation, TU München